The Decadal Mean Ocean Circulation and Sverdrup Balance

Carl Wunsch[1]

22 May 2011

[1]Department of Earth, Atmospheric and Planetary Sciences, Massachusetts Institute of Technology, Cambridge MA 02140 USA, email: cwunsch@mit.edu

ABSTRACT

Elementary Sverdrup balance is tested in the context of the time-average of a 16-year duration time-varying ocean circulation estimate employing the great majority of global-scale data available between 1992 and 2007. The time-average circulation exhibits all of the conventional major features as depicted both through its absolute surface topography and vertically integrated transport stream function. Important small-scale features of the time average only become apparent, however, in the time-average vertical velocity, whether near the surface or in the abyss. In testing Sverdrup balance, the requirement is made that there should be a mid-water column depth where the magnitude of the vertical velocity is less than 10^{-8}m/s (about 0.3m/year displacement). The requirement is not met in the Southern Ocean or high northern latitudes. Over much of the subtropical and lower latitude ocean, Sverdrup balance appears to provide a quantitatively useful estimate of the meridional transport (about 40% of the oceanic area). Application to computing the zonal component, by integration from the eastern boundary is, however, precluded in many places by failure of the local balances close to the coasts. Failure of Sverdrup balance at high northern latitudes is consistent with the expected much longer time to achieve dynamic equilibrium there, and the action of other forces, and has important consequences for ongoing ocean monitoring efforts.

1. Introduction

The very elegant and powerful theories of the time-mean ocean circulation, treated as a laminar flow, remain of intense interest, despite the widespread recognition that the oceanic kinetic energy is dominated by the time variability. As described in many text-books (e.g., Kamenkovich, 1977; Pedlosky, 1996; Vallis, 2006; Huang, 2010), the theories have been the subject of discussion for more than 60 years, and represent a considerable success of theoretical and observational oceanography. Although failing to describe the major kinetic energy regions of the ocean—which are dominated by much smaller spatial scales—the theories have significant skill in reproducing the dominant *potential* energy reservoirs of the ocean (see e.g., Ferrari and Wunsch, 2010, for a discussion of the energy reservoirs and exchanges).

The purpose of this paper is two-fold: (1) to document briefly what is believed to be the best available estimate of the time-average state of the global ocean, 1992-2007 as derived from a combination of most of the oceanographic data that became available during the World Ocean Circulation Experiment (WOCE) and its aftermath; (2) to examine one elementary cornerstone of circulation theory—that of "Sverdrup balance," so as to evaluate the extent to which this construct describes what is perceived of the actual time-mean flow. (The expression "time-mean" is used here as a short-hand for "16-year time average flow" without implying anything about its accuracy relative to conceivable century or even longer time averages.)

2. The time-mean ocean circulation

The ECCO-GODAE[1] project is engaged in estimating the ocean circulation using a family of related general circulation models (GCMs) least-squares fit to the massive global-scale data sets that became available after 1992. This particular version of the MITgcm has 1° lateral resolution and 23 layers. Data used, and the methodology, are described in Wunsch and Heimbach (2007), and on the website http://ecco-group.org. A

[1] Estimating the Circulation and Climate of the Ocean—Global Ocean Data Assimilation Experiment

summary would be that for this very large least-squares problem, Lagrange multipliers are used to enforce the model dynamics and kinematics; descent algorithms are then used to solve the resulting unconstrained problem. The procedure is sometimes known as the "adjoint method," because the model adjoint is used to define the minimizing descent directions. A major advantage of this approach—as compared to what is conventionally called "data assimilation" and which was developed specifically to solve the weather forecasting problem—is that the resulting state estimate satisfies known equations of motion and conservation laws. Solutions can thus be sensibly used to compute heat, vorticity, etc. budgets, not possible with the "jump" solutions used in forecasting.[2] In particular, the estimates, including those used here, come from the *freely running* model subject to the estimated new initial and boundary (meteorological) conditions and so satisfy known equations up to machine precision.

A reviewer asks why the analysis that follows is not being done with a conventional much longer-duration "forward" model output? A summary answer is that one has no way of determining empirically which features of such a model are consistent with observations, and which are not. Many models exist; some are run for hundreds or thousands of years; some features are seemingly realistic; some are not. To what extent do they depict the known (that is observed) system?

Away from the ocean boundaries, and the immediate vicinity of the equator (Eriksen, 1982), the whole ECCO system is dominated by geostrophic, hydrostatic, balance (see Wunsch, 2010a) That is, the system is dominated by the thermal wind and Ekman pumping at the sea surface, and is evolving slowly in time. The classical problem of determining the reference level velocity is automatically solved by the model volume and tracer conservation rules combined with the Ekman forcing. Because these estimates use almost all of the data (altimetric, hydrographic, Argo profiles, scatterometer winds, etc.) that became available nearly globally for the first time in WOCE, they are believed to be

[2]Forecast systems jump at the analysis times when the model state is forced to consistency with the observations, resulting in discontinuities in the budgets for heat, water, momentum, etc.

the most nearly complete rendering of a self-consistent decadal-average global circulation now available. They are not, however, claimed to be "correct," as the data and the model all contain errors, and the coverage for many of the data types (particularly Argo and shipboard hydrography) is both temporally and spatially very inhomogeneous. However, combined with estimates of property transports obtained from parts of this data set (see Ganachaud, 2003, for references), the dominant global elements of the ocean circulation for the 16 years beginning in 1992 are perhaps now known.

The discussion is started with some basic descriptive figures: Figure 1 displays the time mean dynamic topography as calculated from the ECCO version 3.73 estimate. The full range is 2.95 meters from the intense lows in the Southern Ocean to the high in the subtropical gyre of the North Pacific. All of the classically known large-scale features are apparent—including the subtropical and subpolar gyres of the northern hemisphere oceans, and the simpler structures of the southern hemisphere. The Indian Ocean topography is muted because of the averaging of the monsoonal response. To give an indication of the impact of using dynamics, Figure 2 displays the difference between the initial estimate of the mean dynamic topography (taken from Rio and Hernandez, 2004), and the ECCO-GODAE estimate (global spatial means were removed from the fields, as the means have no dynamical influence). Mid-latitude adjustments are O(10cm), reaching 50 cm in small high latitude regions.

Figure 3 displays the transport stream function computed by vertically integrating the zonal flow from top-to-bottom. Note that such an estimate cannot be obtained from observations alone, and requires a dynamical synthesis with a self-consistent GCM. As expected, there are similarities and major differences from the surface topography shown in Figure 1, notably the appearance of the low latitude gyres, and the change in shape of the subtropical gyres. Otherwise, they again conform qualitatively to the classical textbook pictures of the ocean circulation, including e.g., Reid's (1981) "C-shape" of the western North Atlantic circulation. The pattern differences and similarities between Figures 1 and

3 can be interpreted as a simple measure of the importance of the deep flows relative to those manifested at the sea surface. In a gross sense they are similar—with the major gyres and the Antarctic Circumpolar Current being conspicuous in both, although numerous differences also exist, particularly at low latitudes and in the details of the major gyres.

Figure 4 shows the time-mean value of vertical velocity, $w,$ at 117.5 m depth, which is here identified with the mean Ekman pumping velocity, w_E (here "pumping" is defined as the vertical Ekman velocity or either sign, including suction). w_E, unlike the underlying wind-curl, is most directly related to the interior geostrophic flow, a feature perhaps of importance in a model not properly resolving the details of the mixed and Ekman layers. (The wind-stress curl and w_{Ekman} as computed directly from it are shown in Appendix A.) Regions of pumping and suction roughly correspond to the boundaries of the gyres—a tidy, positive, test of conventional theory. The choice 117.5 m is clearly somewhat arbitrary, but is a compromise, for the purposes discussed in the next section, between attempting to define an Ekman layer depth as a complicated function of position and time, and the possibility being explored, of spatially simple dynamical relationships.

At 2000m (Figure 5), the w structure defies easy summary, except to say that high latitudes produce very large values, with the Southern Ocean displaying a complex sign reversal across the Circumpolar Current, whose reliability with a 1° lateral resolution model is doubtful. The persistence of spatial scales much smaller than the gyres over the entirety of the ocean is consistent with the inference (see Wunsch, 2010b) that no low frequency cutoff exists in the high wavenumber structures appearing in the ocean circulation. Human eyes are captured by the large-scale patterns in figures such as 1 or 4, and do not readily detect the important smaller scales having strong spatial derivatives (see also, Lu and Stammer, 2002).

A full description of these results requires a discussion of the global general circulation and all of its regionally varying physics—an undertaking far beyond what is intended here. Instead, we use them as a backdrop for discussion of the special element of the

circulation known as Sverdrup balance (SB).

3. Sverdrup balance (SB)

a. Background

SB is one of the cornerstones of ocean dynamics and much of the theory of the ocean circulation is built directly on the assumption of its accuracy. Ever since Sverdrup's (1947) demonstration in the tropical Pacific Ocean of its apparent utility, it's appeal has been plain: it attempts to represent the meridional (and secondarily) the zonal mass or volume transports employing only the *local* wind-stress in a linear dynamical framework. Every oceanographic textbook discusses SB as the major explanatory feature of the steady circulation as depicted in figures such as 1-5.

Despite its central role, surprisingly little effort has been expended in attempting to understand quantitatively the extent to which SB does describe the circulation (Wunsch, 1996, Ch. 2 provides a review of efforts to that time). A first attempt at doing so was that of Leetmaa *et al.* (1977), and which inspired the study of Wunsch and Roemmich (1985). The Leetmaa *et al.* (1977) test was an integral one, showing that a level-of-no-motion could be chosen in the North Atlantic at 25°N in such a way that the zonally integrated southward flow above the reference level was nominally equal to the measured transport at that latitude of the Gulf Stream. It was assumed that the net southward flow arose because of SB. Wunsch and Roemmich (1985) argued that: (1) the balance involved an extrapolation across the Gulf Stream recirculation, where the evidence was against the existence of any level-of-no-motion; (2) that the implied meridional heat transport would be far too small for consistency with other estimates; and (3) that the induced bottom vertical velocities in the abyssal North Atlantic would dominate the surface-Ekman-pumping velocities implicit in Sverdrup balance. Note however, that failure of a basin-wide integral test does not preclude the possibility of the accuracy of the balance at individual points or over large regions. Schmitz *et al.* (1992) revisited the question, inferring that balancing the upper

ocean mass transports was not reasonable—given also the water mass characteristics of the Gulf Stream deriving from the southern hemisphere. Subsequently, Hautala *et al.* (1994) concluded that SB did have some validity in the Pacific Ocean, testing it at 24°N in an integral manner analogous to that of Leetmaa *et al.* (1977). Here I explore the possibility of point-balance, on a global scale, rather than zonally integrated skill. The applicability of SB has been discussed in passing, regionally, often in near-boundary regions, by numerous authors (e.g., Qiu and Joyce, 1992)—but which are not reviewed here.

The most basic derivation of SB assumes the validity of the geostrophic vorticity equation,[3]

$$\beta v = f \frac{\partial w}{\partial z}, \tag{1}$$

in a regime of low Rossby and Ekman number, and which when integrated, leads to,

$$\int_{z_0}^{\eta} v\left(x,y,z,t\right) dz = \beta V_g\left(x,y,t\right) = f\left(w\left(x,y,z=0\right) - w\left(x,y,z_0\right)\right). \tag{2}$$

Here V_g is the geostrophic component, only. Elementary Ekman layer theory produces,

$$w_E = w\left(z=0\right) = \hat{\mathbf{k}} \cdot \nabla \times \left(\boldsymbol{\tau}/\rho_0 f\right), \tag{3}$$

where it is understood that $w\left(z=0\right)$ is evaluated at the base of the Ekman layer, not the actual sea surface. Then Eq. (2) produces,

$$V_g\left(x,y,t\right) = f w_E/\beta,$$

if $w\left(z_0=0\right)$. The *total* meridional transport, $V = V_g + V_E$, where V_E is the meridional

[3]Sverdrup (1947) never used this equation. It was only much later that the explicit connection between SB and Ekman pumping came to be recognized. Sverdrup did state explicitly that he was assuming $u = v = w = 0$ at $z = z_0$.

component of the Ekman transport, and thus becomes the textbook version,

$$\beta V(x,y,t) = \hat{\mathbf{k}} \cdot \nabla \times \boldsymbol{\tau}(x,y,t) / \rho_0, \tag{4}$$

again *assuming* $w(z_0) = 0$. Notation is purely conventional, with β being the meridional derivative of the Coriolis parameter, $\boldsymbol{\tau}$, the vector wind-stress, V, and V_g, the meridional mass or volume transports (not distinguished) and $\hat{\mathbf{k}}$ is the unit vertical vector. ρ_0 is a constant reference density. Spherical coordinates are readily substituted if desired, and the variations of ρ are optionally accounted for at the level of accuracy available now. A rigorous derivation of Eq. (4) requires some care (Fofonoff, 1962; Pond and Pickard, 1983). Many of the older discussions of SB are based upon the outdated assumption that abyssal and bottom velocities, and hence their divergences and stresses, are negligible.

A more complete analysis (following Fofonoff, 1962) would integrate to the sea floor, where the value of $w(x,y,z=-h)$ would take the place of $w(x,y,z_0)$, the procedure used e.g., by Luyten *et al.* (1985) and Lu and Stammer (2002). This approach becomes a test not of SB per se, but of the applicability of geostrophic vorticity balance, and is not attempted here, because the abyssal circulations in all models are suspect for a number of reasons. These reasons include the failure to include a spatially varying abyssal vertical mixing scheme, which can have a profound effect on local deep values of w, and because the spin-up of the model abyssal ocean is almost surely incomplete.

No theory predicts the value of z_0, if it exists, and several choices have been used in the literature including fixed depths and isopycnals. The choice of integration depth is an important factor in the differences in the results of these studies. Furthermore, none of the standard choices can be justified, or is expected to be globally applicable. To the extent that z_0 is a free parameter, permitted to vary spatially in an arbitrary fashion, any kind of statistical test becomes nearly impossible, as would also be true if the definition depth of w_E were permitted to vary.

Other difficulties, only slightly less fundamental, arise including, especially, the ques-

tion of whether t in Eq. (4) is instantaneous (applying to synoptic motions), or denotes e.g., the middle of a long-averaging interval. In most analyses of concern here, and as in Sverdrup (1947), it is the latter that is either assumed or implied. But how long an averaging interval is long enough? Answering that question can be tackled by analyzing the theoretical temporal response of the ocean. One can attempt to answer it empirically, but only if records are long enough. A number of investigators have discussed "time-dependent Sverdrup balance" in which the considerations of integration depth are quite different (see e.g., Anderson *et al.,* 1979; Sturges and Hong, 1995). The time-dependent problem becomes a discussion of baroclinic Rossby and Kelvin, etc., wave responses, their dissipation times, and of their interactions with the "mean" flow. Adjustment times would be a strong function of latitude, far shorter at low than at high latitudes. Various wind field products have also been used over the years, and some of them have known significant errors (e.g., Josey *et al.,* 2002; cf. Townsend *et al.,* 2000). In this present case, the wind field used is derived from the NCEP-NCAR reanalysis estimate plus the NSCATT data, but significantly modified to bring the ocean into accord with the large number of oceanic observations (Wunsch and Heimbach, 2007).

Direct observation of w in the ocean has not been possible, and even in most models, w is so noisy as to be awkward to analyze (see Lu and Stammer, 2002). Consequently, many investigators with observations assumed, instead, that it was a level-of-no-horizontal motion, where $v\,(z_0)$ was claimed to vanish, although that would correspond to the depth where $\partial w/\partial z$ vanished instead of w. (If, as used to be assumed, the abyss below z_0 were truly at rest, both would then vanish.)

Figure 6 is an example of a profile of $w\,(z)$ where a mid-water column sign change does occur. This particular profile corresponds to the classical picture of a subtropical gyre region of Ekman pumping above a region of upwelling. Figure 7 is a near-global chart of the depth where w reaches a minimum, and Figure 8 displays the value of the minimum velocity. Large velocity magnitudes are found in the Southern Ocean (which, as always,

proves exceptional), at high northern latitudes and in the vicinity of the strong boundary currents. In those places, one would expect simple SB to fail, and we exclude them in what follows. (The controversy over SB in the Southern Ocean is discussed by Olbers, 1998. Mazloff *et al.*, 2010, discuss state estimates there.)

The practical difficulties of defining SB could lead to the conclusion that it is not a particularly useful description of the ocean circulation. On the other hand, it is both a powerful simplifying tool, and a compelling descriptor. Where the complexity of oceanic flows often tends to defy verbal description, one is loathe to simply abandon it. If the only quantitative description of the oceanic general circulation must be the space and time varying flow at each grid point of a high resolution model, a great deal is lost.

We will make the hypothesis that a 16-year averaging time is sufficient to produce flows satisfying the basic SB, and test it. Some feeling for the large-scale time-mean flows in this estimate can be gained from the figures appearing above.

b. Determining an integration depth

Let $\tilde{v}$ be the value predicted from the model vertical velocity profiles,

$$\tilde{v}\left(x,y,z\right)=\frac{f}{\beta}\frac{\partial\tilde{w}\left(x,y,z\right)}{\partial z}. \tag{5}$$

From here on, all symbols refer to the 16-year time average and the tildes, denoting an estimate, will be omitted.

w is very noisy, even as a 16 year, spatially-smoothed, time-average (Figure 5). A 5° of latitude and longitude spatial average has been used in the following calculations—as a way of partially suppressing the grid-scale noise in w, and which is present in all finite difference models of this type. A 5° averaging distance is arbitrary, but appears to be a reasonable compromise between displaying regional structures and the suppression of noise.

The first question is whether any depth z_0 exists—such that $w\left(x,y,z_0\left(x,y\right)\right)\approx 0$

below the region where Ekman layer physics might be thought to apply, but above the bottom? To answer that question a search was conducted to find the depth of the minimum value of $|w(x,y,z_{\min})|$ over the whole domain, with result shown in Figure 7. Over much of the ocean, such a depth is found to lie between about 1000-1500m depth, and suggesting its potential utility. Thus, the value of $w(x,y,z_{\min})$ is displayed in Figure 8.

c. Testing the relationship

We take as candidates for useful SB those regions where the spatially smoothed value of $|w(x,y,z_{\min})| < 10^{-8}$ m/s. This choice is also arbitrary, being equivalent to a vertical displacement bound of about 0.3m/y. The notion is to test, at each point,

$$\int_{z_{\min}}^{0} v(x,y,z)\,dz = V_g(x,y) = \frac{f}{\beta} w(x,y,z=-117\text{m}) = \frac{f}{\beta} w_E(x,y)$$

where $w(x,y,-117m)$ is assumed to represent the Ekman pumping or suction, noting that V includes the Ekman-transport. This test is a compromise between using the most basic relationship, Eq. (1) and the derived version Eq. (4). The test used is to form the normalized difference,

$$\varepsilon(x,y) = \frac{f/\beta w_E(x,y) - V_g(x,y)}{+|f/\beta w_E(x,y)| + |V_g(x,y)|},$$

and which would vanish if SB were perfect and is bounded by ± 1. The result is shown in Figure 10. Lines of low-latitude vanishing wind-stress curl ($w_E = 0$) are conspicuous there, as is a failure at and near the equator (compare to Figure 4). Over the subtropical gyres of all oceans however, the fit is within about 20%, and thus one might well conclude that there is considerable skill. Failure to find applicability at high northern latitudes is consistent with the much longer adjustment times expected there from the theoretical calculation of Veronis and Stommel (1956) and as recomputed here in Figure 9. Sixteen years is far too short to expect an equilibrium response at high latitudes (with the Southern Ocean being anomalous in many other ways, too) even should the forcing become quasi-

steady. The radically different temporal adjustment times of high and low latitudes and the very different structures of the time-varying windfields, make it unlikely, a priori, that there should be any simple large-scale structure encompassing both.

Figure 11 is the unnormalized difference in Sverdrups, and which over the regions of apparent validity, produces agreement within about 0.1Sv per 100 km of zonal distance. Generally speaking the interior subtropical gyres appear to be in SB, as do tropical circulations away from the equator itself (where the conventional w_E is undefined). The Indian Ocean seems to show some accuracy, but confined to the interior well-east of the African coast. Roughly 40% of the oceanic area appears consistent with SB.

Notice that basin-wide integral tests such as those used by Leetmaa *et al.* (1977) will fail in the North Atlantic, as the relationship is inaccurate both toward eastern and western boundaries. It does have some useful point-wise (or 5° area-average) utility there. On the other hand, in the low latitude North Pacific, such as the 24°N latitude used by Hautala *et al.* (1994), there is reasonable accuracy close to the eastern boundary, and the integral test should, as they found, be satisfied. A similar positive result appears in the low-latitude South Atlantic.

4. Discussion

Studies such as this one raise more questions than they answer. The simplest inference is that over the interiors of subtropical and tropical gyres of the ocean, ordinary Sverdrup balance (SB) produces a quantitatively useful description of the meridional mass or volume transports in a 16-year average estimate. In those regions, the purely local time-average wind stress curl has a significant skill in predicting the meridional motions in the upper ocean. Calculation of the zonal component of flow is not, however, mostly possible, given the failure of the basic balance in V_g to be applicable over complete zonal sections, with the low latitude South Atlantic and Pacific Oceans being exceptions.

Among the imponderables here is whether a much longer time average (centuries?)

would expand the region of apparent skill? Whether the meteorology is sufficiently stable over that period to produce such equilibrium balances is also quite unknown. The very long memory/adjustment time of the deep ocean would also need to be accounted for. As it is, the lack of applicability of SB north of about 45°N is consistent with the expected multi-decadal time scales for linear baroclinic adjustment there—16 years is probably far too short to obtain an equilibrium result, even if the forcing were steady and only the wind stress were acting (see Figure 9, or Sturges and Hong, 1995). The situation is made even more complex by the small-scale structures apparent at high northern latitudes in the Ekman pumping (Figure 4). The Southern Ocean south of about 30°S has a different physics.

The presence of small scale structures in all elements of the flow, including deviations from SB, is consistent with the inference (Wunsch, 2010b) that significant elements of mesoscale variability persist at the longest accessible time scales. What does emerge here is that Sverdrup balance does have some quantitative analytical skill over large parts of the ocean, and can thus be used as a descriptive statement there. It partially rationalizes the structures in Figs. 1 and 3 in particular regions, but neither is simply related to the actual SB-driven flow, as one is a surface manifestation, the other a whole water column integral. On the other hand, the inability to use SB in many regions, even after averaging for 16 years, means that much of the most interesting and important regions of the oceans at high latitudes everywhere present a continuing serious theoretical and descriptive challenge. Observational programs attempting to monitor the behavior of the entire ocean through latitudinally sparse measurement systems confront very different time scales and equilibrium times over the globe. The simplest linear dynamics (Fig. 9) shows that low latitude oceanic responses to disturbances are unlikely to be simply related to high latitude ones. These same ECCO results (Wunsch, 2011) display no linear correlations between subtropical and subpolar fluctuations in the meridional overturning—consistent with that simple theory. Whether averaging times of many decades would show such correlations

remains unknown (cf. Bingham et al., 200x).

This study can be extended and possibly improved in a number of ways, and no claim is made that it is definitive: as more data accumulate, longer time intervals can be explored; regions of intense eddies, when properly depicted by constrained eddy-resolving models, may change the results, at least regionally; a spatially varying depth of definition of w_E might conceivably improve the results; particular unconstrained models will likely give different answers. But as was stated at the beginning, the goal here was to ask whether a particular dynamical relationship, Sverdrup balance, if defined in as simple a way as was reasonable, would be found to have quantitative skill in describing the observed ocean circulation? The answer is "yes," over a major portion of the observed ocean.

Acknowledgments. Supported in part by the ECCO-GODAE project (NASA Contract NNX09AI87G) and the North Atlantic Meridional Overturning Experiment (NASA NNX08AV89G). J. Holt carried out a number of useful preliminary calculations. I had much help with data handling from C. King and D. Spiegel. I thank B. Klinger for inspiring Figure 3, and R. Ponte and P. Heimbach and two anonymous referees for helpful comments.

Appendix A. Wind Stress Curl

The ECCO-GODAE solutions are derived from a GCM driven by adjusted meteorological fields, where the adjustments are those required to bring the model into consistency within estimated errors of the oceanic observations. Thus, among other fields, the wind stresses differ from those in the initial estimates of the values of those fields (in this particular case, derived from the combined NCEP-NCAR reanalyses and the NSCATT). For reference and reassurance, we display here the meridional transports $V = \left(\hat{\mathbf{k}} \cdot \nabla \times \boldsymbol{\tau}/\rho_0\right)/\beta$ in Figure 12, and the Ekman velocity, computed directly, $w'_E = \hat{\mathbf{k}} \cdot \nabla \times (\boldsymbol{\tau}/\rho_0 f)$, (e.g., Gill, 1982; or Huang, 2010). These are quantitatively very similar to e.g., similar figures published by Chelton *et al.* (2004) from the scatterometer and Figure 4 above. The Chelton *et al.* (2004) averaging time was different (four years) and note too, that the scatterometer data were used on a daily basis as part of the ECCO-GODAE initial-estimate forcing fields and so are not independent estimates. Some discussion of the complexity of the situation in the Southern Ocean can be found e.g., in Mazloff *et al.* (2010).

In the tests of SB, w_E (see Figure 4) was taken from the model estimate at 117.5m, which has no equatorial singularity, and is directly related to the geostrophic flow, V_g, beneath, not involving the meridional Ekman transports implicit in V.

References

Anderson, D. L. T., K. Bryan, A. E. Gill, and R. C. Pacanowski, 1979. Transient-response of the North Atlantic - some model studies. J. Geophys. Res., *84*, 4795-4815.

Bingham, R. J., C. W. Hughes, V. Roussenov, and R. G. Williams, 2007. Meridional coherence of the North Atlantic meridional overturning circulation. Geophys. Res. Lett., *34*.

Chelton, D. B., R. A. deSzoeke, M. G. Schlax, K. El Naggar, N. Siwertz, 1998. Geographical variability of the first baroclinic Rossby radius of deformation. J. Phys. Oc., *28*, 433-460.

Chelton, D. B., M. G. Schlax, M. H. Freilich, and R. F. Milliff, 2004. Satellite measurements reveal persistent small-scale features in ocean winds. Science, *303*, 978-983.

Eriksen, C. 1982. Geostrophic equatorial deep jets. J. Mar. Res, *40*, 143?157.

Ferrari, R. and C. Wunsch, 2010. The distribution of eddy kinetic and potential energies in the global ocean. Tellus A, *62*, 92-108.

Fofonoff, N. P. 1962. Dynamics of ocean currents, *in* The Sea, Vol. 1, 323-395, Wiley-Interscience, New York.

Frankignoul, C., P. Müller, and E. Zorita, 1997. A simple model of the decadal response of the ocean to stochastic wind forcing. J. Phys. Oc., *27*, 1533-1546.

Ganachaud, A. 2003. Large-scale mass transports, water mass formation, and diffusivities estimated from World Ocean Circulation Experiment (WOCE) hydrographic data. J. Geophys. Res., *108*, 3213.

Gill, A. E. 1982. Atmosphere-Ocean Dynamics, Academic Press, New York, 662pp.

Hautala, S., D. Roemmich, and W. J. Schmitz Jr, 1994. Is the North Pacific in Sverdrup balance along 24°N. J. Geophys. Res, *99*, 16,041-16,052.

Huang, R. X. 2010. Ocean Circulation: Wind-driven and Thermohaline Processes, Cambridge; New York, Cambridge University Press, 791pp.

Josey, S. A., E. C. Kent, and P. K. Taylor, 2002. Wind stress forcing of the ocean in the

SOC climatology: Comparisons with the NCEP/NCAR, ECMWF, UWM/COADS, and Hellerman and Rosenstein datasets. J. Phys. Oc., *32*, 1993-2019.

Kamenkovich, V. M. 1977. Fundamentals of Ocean Dynamics, Elsevier, Amsterdam, 249pp.

Leetmaa, A., P. Niiler, and H. Stommel, 1977. Does the Sverdrup relation account for the mid-Atlantic circulation? J. Mar. Res., *35*, 1-10.

Lu, Y. and D. Stammer, 2004. Vorticity balance in coarse-resolution global ocean simulations. J. Phys. Oc., *34*, 605-622.

Luyten, J., H. Stommel, H. and C. Wunsch, 1985. A diagnostic study of the northern Atlantic subpolar gyre. J. Phys. Oc., *15*, 1344-1348.

Mazloff, M. R., P. Heimbach, and C. Wunsch, 2010. An eddy-permitting Southern Ocean state estimate. J. Phys. Oc., *40*, 880-899.

Olbers, D. 1998. Comments on "On the obscurantist physics of 'form drag' in theorizing about the Circumpolar Current". J. Phys. Oc., *28*, 1647-1654.

Pedlosky, J. 1996. Ocean Circulation Theory, Berlin, Springer, 453pp.

Pond, S. and G. L. Pickard, 1983. Introductory Dynamical Oceanography, second edition, Pergamon, Oxford, 329pp.

Qiu, B. and T. M. Joyce, 1992. Interannual variability in the midlatitude and low-latitude western North Pacific. J. Phys. Oc., *22*, 1062-1079.

Reid, J. L. 1981. On the mid-depth circulation of the world ocean, *in* Evolution of Physical Oceanography, B. A. Warren and C. Wunsch, Eds., 70-111,The MIT Press (available online by search at http://web.mit.edu).

Rio, M. H. and F. Hernandez, 2004. A mean dynamic topography computed over the world ocean from altimetry, in situ measurements, and a geoid model. J. Geophys. Res., *109*.

Roquet, F. and C. Wunsch, 2011. On the patterns of wind-power input to the ocean circulation. Submitted for publication.

Schmitz , W. J., J. D. Thompson, and J. R. Luyten, 1992. The Sverdrup circulation for the Atlantic along 24°N. J. Geophys. Res.-Oceans, *97*, 7251-7256.

Sturges, W. and B. B. Hong, 1995. Wind forcing of the Atlantic thermocline along 32°N at low-frequencies. J. Phys. Oc., *25*, 1706-1715.

Sverdrup, H. 1947. Wind-driven currents in a baroclinic ocean; with application to the equatorial currents of the eastern Pacific. Proc. Natl. Acad. Scis. USA, *33*, 318.

Townsend, T. L., H. E. Hurlburt, and P. J. Hogan, 2000. Modeled Sverdrup flow in the North Atlantic from 11 different wind stress climatologies. Dyn. Atm. Oceans, *32*, 373-417.

Vallis, G. K. 2006. Atmospheric and Oceanic Fluid Dynamics: Fundamentals of Large-scale Ciculation, Cambridge Un. Press, Cambridge, 745pp.

Veronis, G. and H. Stommel, 1956. The action of variable wind stresses on a stratified ocean. J. Mar. Res., *15*, 43-75.

Wunsch, C. 2010a. Variability of the Indo-Pacific Ocean exchanges. Dyn. Atm. and Oceans, *50*, 157-173.

Wunsch, C. 2010b. Towards a mid-latitude ocean frequency-wavenumber spectral density and trend determination. J. Phys. Oc., *40*, 2264-2281.

Wunsch, C., 2008. Mass and volume transport variability in an eddy-filled ocean. Nature Geosci., 1, 165-168.

Wunsch, C., 2011. Covariances and linear predictability of the North Atlantic Ocean. Submitted for publication.

Wunsch, C. and P. Heimbach, 2006. Estimated decadal changes in the North Atlantic meridional overturning circulation and heat flux 1993-2004. J. Phys. Oc., *36*, 2012-2024.

Wunsch, C. and P. Heimbach, 2007. Practical global oceanic state estimation. Physica D-Nonlinear Phenomena, *230*, 197-208.

Wunsch, C. and D. Roemmich, 1985. Is the North Atlantic in Sverdrup balance? J. Phys.

Oc., *15*, 1876-1880.

Figure Captions

1. Absolute mean dynamic topography relative to the geoid in meters of the 16-year average of the ECCO estimate known as version 3.73.

2. Difference (in meters) of the sea surface elevation, η, in the final state estimate, from the initial estimate of Rio and Hernandez, (2004). The adjustments are the result of the use of all data and model dynamics. Contour interval is 5 cm and negative areas are in gray.

3. Transport stream function in 10^6 m^3/s from the 16-year average. Some of the contours in the high latitude Southern Ocean have been omitted. The function is set to zero on the western boundaries (from a code of B. Klinger).

4. $10^6 w\,(z = -117.5 \text{ m})$ in m/s. Regions of suction $(w_E > 0)$ and pumping ($w_E < 0$) are distinct but noisy even after 16 years of averaging. The regions of equatorial upwelling (not an Ekman velocity), and subtropical gyre downward pumping are conspicuous. Complex structures at high latitudes are not discussed in this paper nor is the non-Ekman flow on the equator. Note the non-uniform contour intervals. White curve denotes the zero contour. Compare to Fig. 13 in the Appendix.

5. Estimated 16 year average $10^7 w\,(x, y, z)$ in m/s at $z = 2000$ m smoothed over 5° areas of latitude and longitude. Contour interval is 50 in units of 10^7m/s. Gray areas are negative (downwards). Isolated extreme regions of both signs occur only in the Southern Ocean and high northern latitudes.

6. $v\,(50°\text{W}, 30°\text{N}, z)$, solid curve, (left panel) as well as its value when multiplied by Δz (middle panel). $w\,(z)$ (right panel) showing that in this case, there is a depth (arrow) where $w\,(z_0) = 0$, and chosen as the depth to use in putative Sverdrup balance. The point and horizontal average values are visually indistinguishable here.

7. The depth $z_{\min}$ where $|w|$ reaches its minimum value. Small regions where $z_{\min} < 500$ m, or > 4000 m would be suspect.

8. $10^8 w\,(x, y, z_{\min})$–the value of w, with sign, at the depth of its minimum absolute

value in m/s. Negative regions are gray. Contour interval is 50 in units of 10^8 m/s.

9. Integral of $v(x,y,z)\Delta x$ from 0m to $z_{w\min}$ in Sverdrups, for each degree of longitude, smoothed over 5 degrees of latitude and longitude. Δx is the longitudinal grid spacing, and which is a function of latitude.

10. The time required for a first-mode baroclinic Rossby wave signal to cross the North Atlantic Ocean. Computed as $L(y) / (\beta(y) R_d^2(y))$, where $L(y)$ is the ocean width, and $R_d(y)$ is the zonal average first baroclinic mode deformation radius value from Chelton et al. (1998). Despite the poleward narrowing of the ocean, the reduction in both β and R_d greatly increases the adjustment time with latitude. Note that equilibrium times would be far longer.

11. The normalized difference$(f/\beta w_E - V_g) / (|f/\beta w_E| + |V_g|)$ in Sverdrups per degree of zonal separation where the absolute value is less than 0.1 Sv and $|w_{\min}| < 10^{-8}$m/s. Regions of both signs of w_E pass the test of sufficiently small values. No equatorial singularity is seen seen as w_E is taken to be its value at $z = -117.5$m and the flow right at the equator is the absolute transport, not the geostrophic one.

12. The difference $f/\beta w_E - V_g$ in Sverdrups per degree of zonal separation where the absolute value is less than 0.1Sv and $|w_{\min}| < 10^{-8}$m/s. (Same as Fig. 10 except that the difference is not normalized.)

13. Mean wind stress curl, $(\Delta x/\rho_0\beta)\,\nabla\times\boldsymbol{\tau}$**,** in Sverdrups, averaged over 5° of latitude and longitude. Values are from the ECCO-adjusted winds.

14. $10^6\hat{\mathbf{k}}\cdot\nabla\times(\boldsymbol{\tau}/\rho_0 f)$ m/s, the Ekman pumping velocity as computed directly from the ECCO adjusted wind stress (m/s). Equatorial singularity has been suppressed. Compare to Fig. 4.

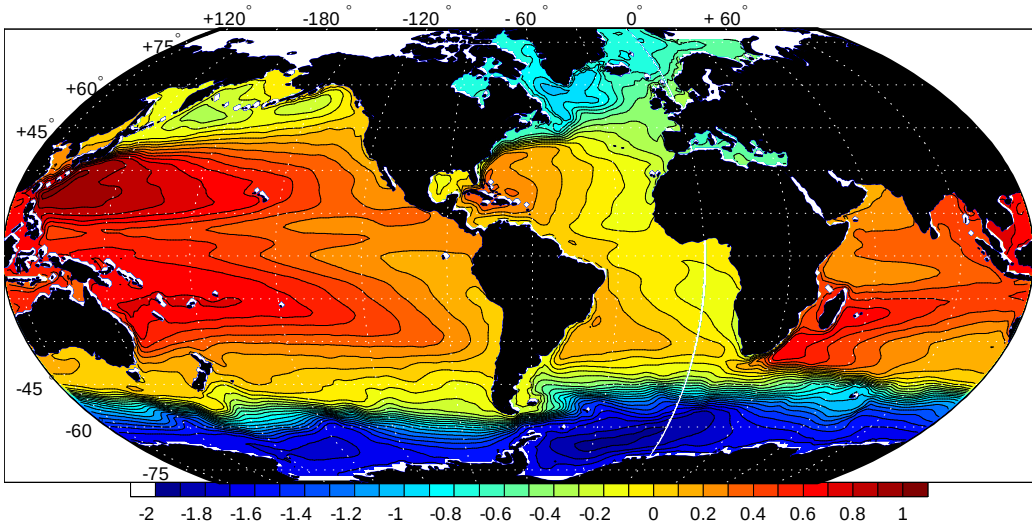

Figure 1: Absolute mean dynamic topography relative to the geoid in meters of the 16-year average of the ECCO estimate known as version 3.73.

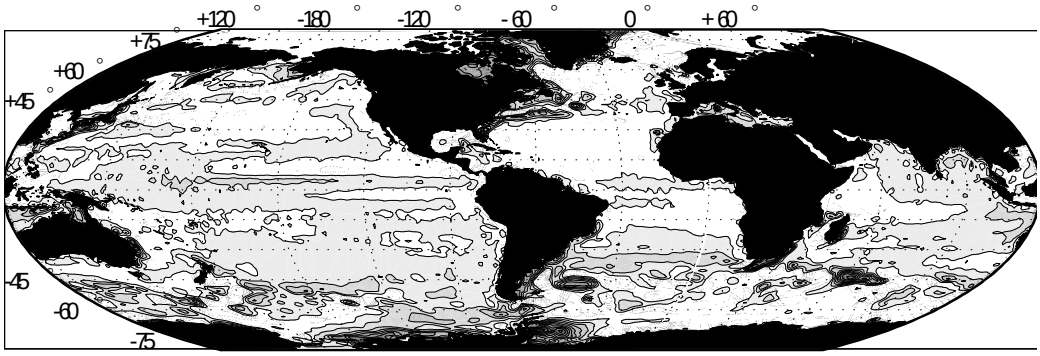

Figure 2: Difference (in meters) of the sea surface elevation, η, in the final state estimate, from the initial estimate of Rio and Hernandez, (2004). The adjustments are the result of the use of all data and model dynamics. Contour interval is 5 cm and negative areas are in gray.

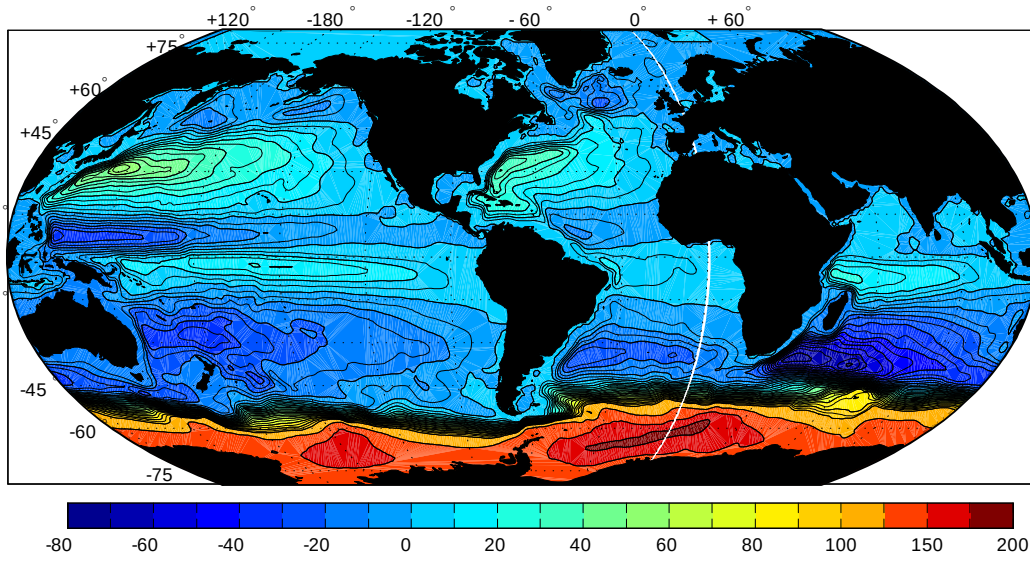

Figure 3: Transport stream function in 10^6 m^3/s from the 16-year average. Some of the contours in the high latitude Southern Ocean have been omitted. The function is set to zero on the western boundaries (from a code of B. Klinger).

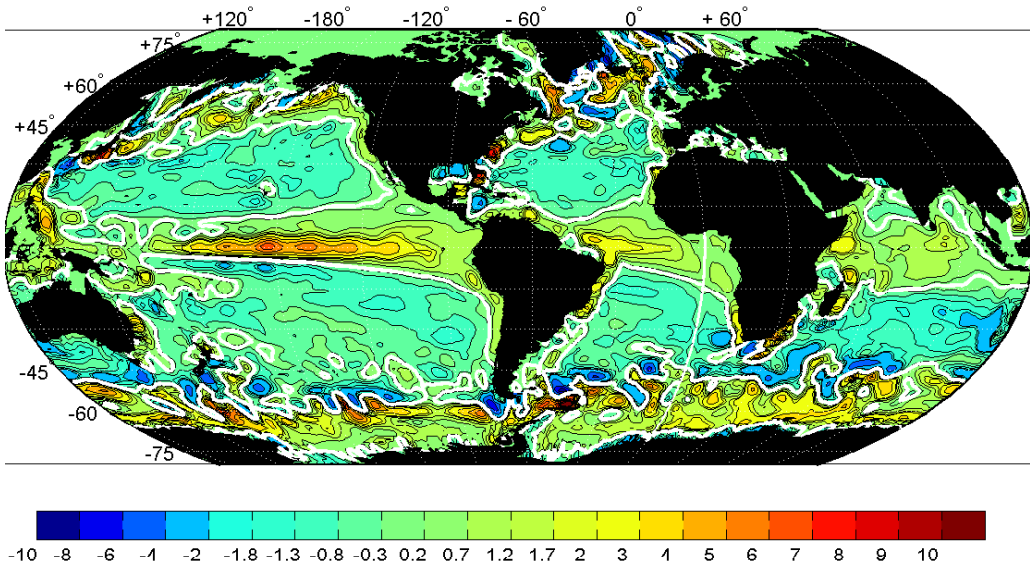

Figure 4: $10^6 w\,(z = -117.5\,\mathrm{m})$ in m/s. Regions of suction $(w_E > 0)$ and pumping ($w_E < 0$) are distinct but noisy even after 16 years of averaging. The regions of equatorial upwelling (not an Ekman velocity), and subtropical gyre downward pumping are conspicuous. Complex structures at high latitudes are not discussed in this paper nor is the non-Ekman flow on the equator. Note the non-uniform contour intervals. White curve denotes the zero contour. Compare to Fig. 13 in the Appendix., noting the different ranges and colorbars.

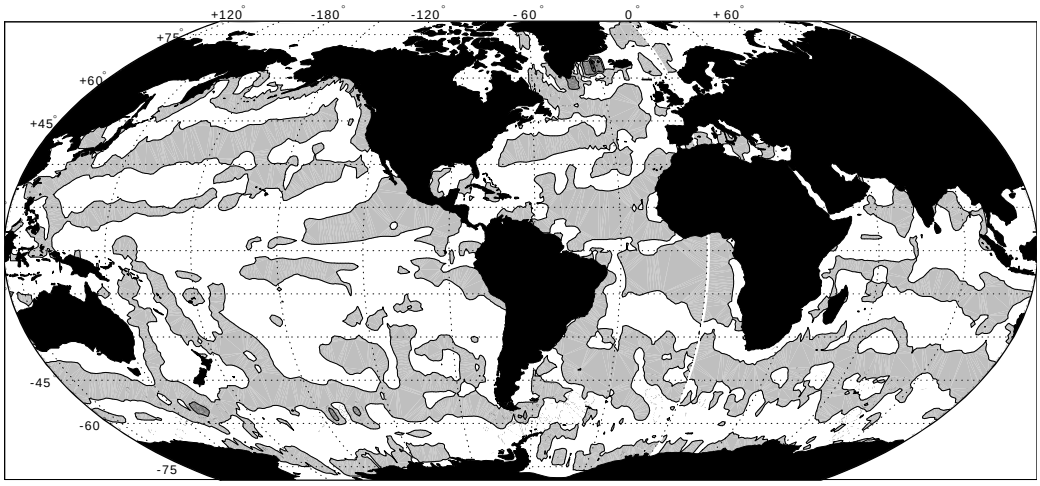

Figure 5: Estimated 16 year average $10^7 w\left(x,y,z\right)$ in m/s at $z=2000$ m smoothed over 5° areas of latitude and longitude. Contour interval is 50 in units of 10^7m/s. Gray areas are negative (downwards). Isolated extreme regions of both signs occur only in the Southern Ocean and high northern latitudes.

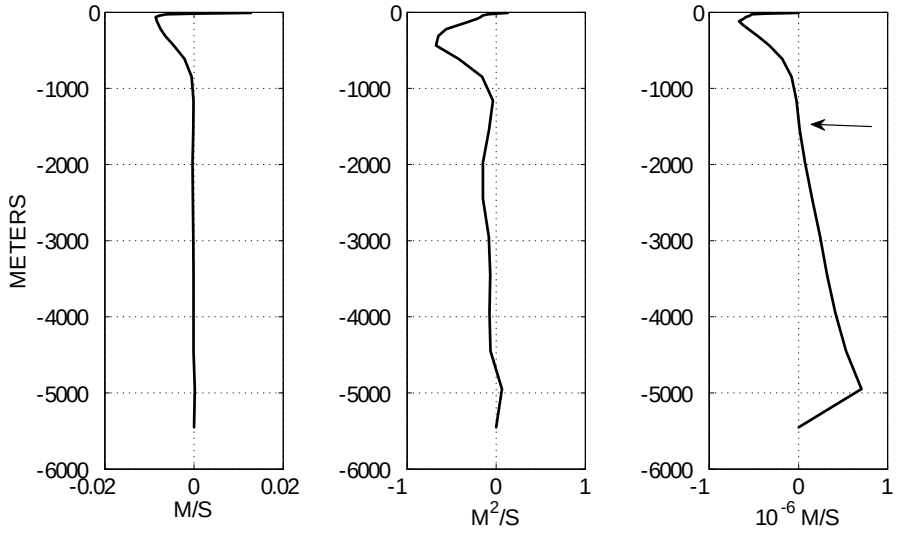

Figure 6: $v\left(50^{\circ}\text{W},30^{\circ}\text{N},z\right)$, solid curve, (left panel) as well as its value when multiplied by Δz (middle panel). $w\left(z\right)$ (right panel) showing that in this case, there is a depth (arrow) where $w\left(z_0\right)=0$, and chosen as the depth to use in putative Sverdrup balance. The point and horizontal average values are visually indistinguishable here.

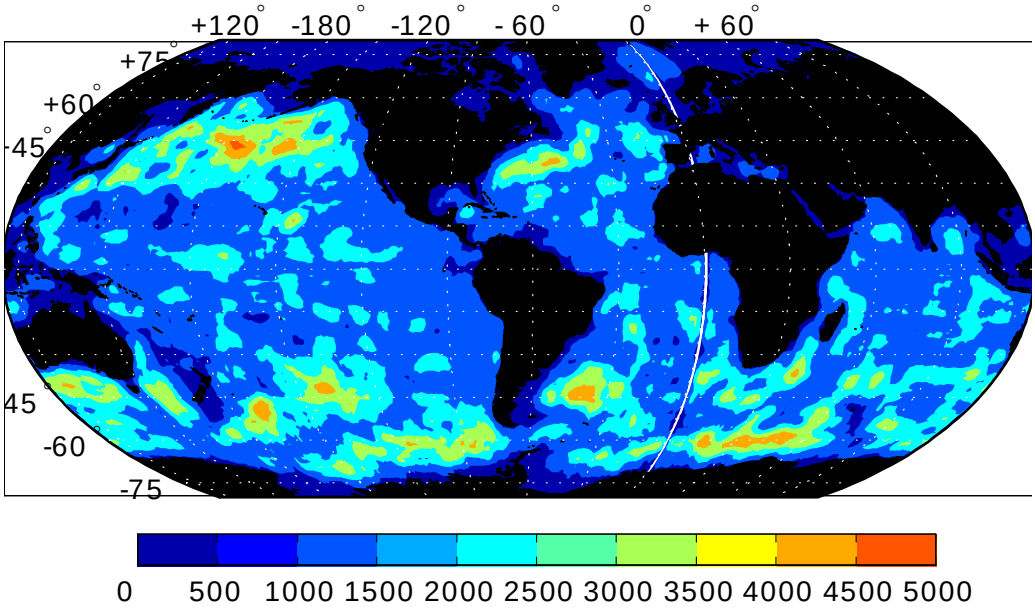

Figure 7: The depth $z_{\min}$ where $|w|$ reaches its minimum value. Small regions where $z_{\min} < 500$ m, or > 4000 m would be suspect.

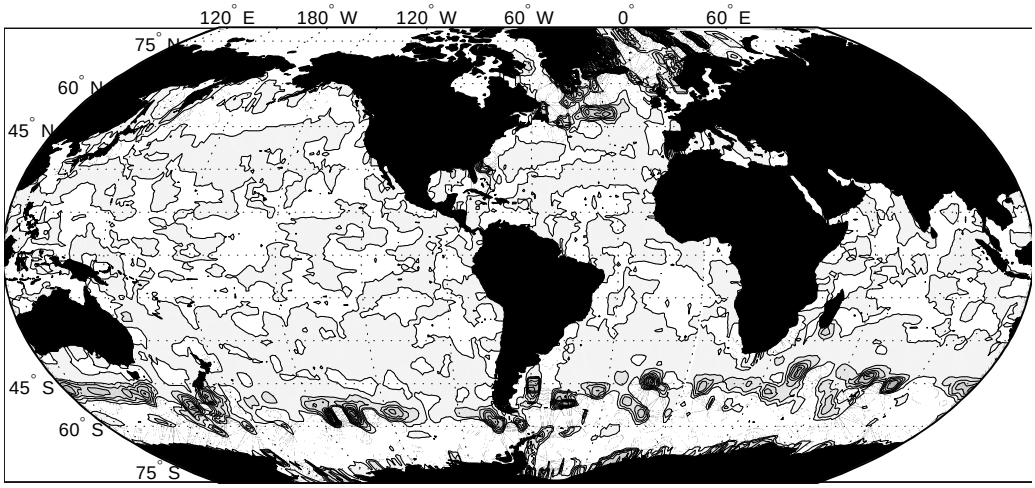

Figure 8: $10^8 w\,(x, y, z_{\min})$–the value of w, with sign, at the depth of its minimum absolute value in m/s. Negative regions are gray. Contour interval is 50 in units of 10^8 m/s.

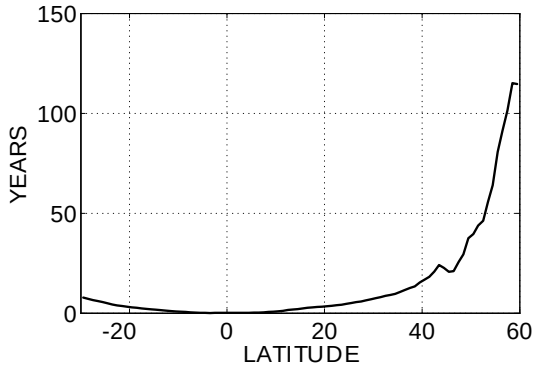

Figure 9: The time required for a first-mode baroclinic Rossby wave signal to cross the North Atlantic Ocean. Computed as $L(y) / (\beta(y) R_d^2(y))$, where $L(y)$ is the ocean width, and $R_d(y)$ is the zonal average first baroclinic mode deformation radius value from Chelton et al. (1998). Despite the poleward narrowing of the ocean, the reduction in both β and R_d greatly increases the adjustment time with latitude. Note that equilibrium times would be far longer.

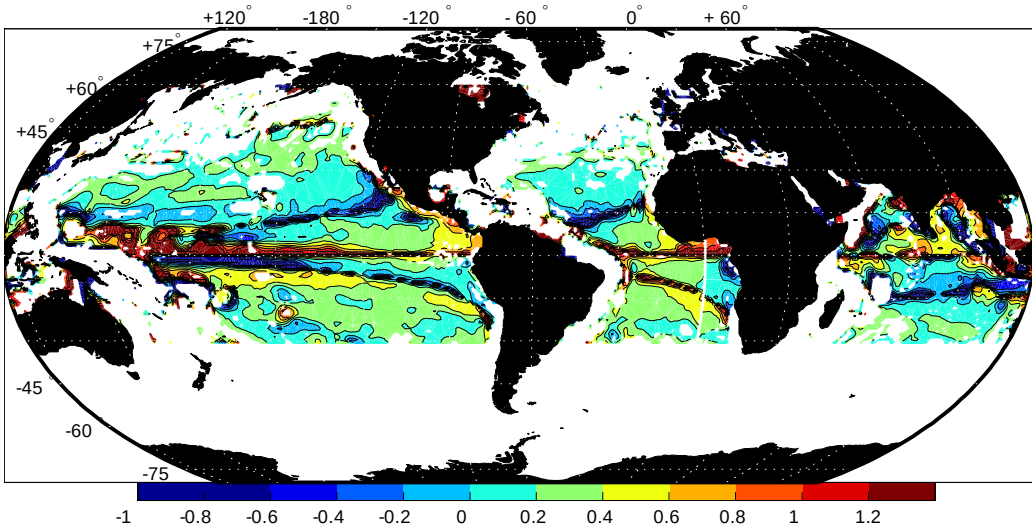

Figure 10: The normalized difference$(f/\beta w_E - V_g) / (|f/\beta w_E| + |V_g|)$ in Sverdrups per degree of zonal separation where the absolute value is less than 0.1 Sv and $|w_{\min}| < 10^{-8}$m/s. Regions of both signs of w_E pass the test of sufficiently small values. No equatorial singularity is seen seen as w_E is taken to be its value at $z = -117.5$m and the flow right at the equator is the absolute transport, not the geostrophic one.

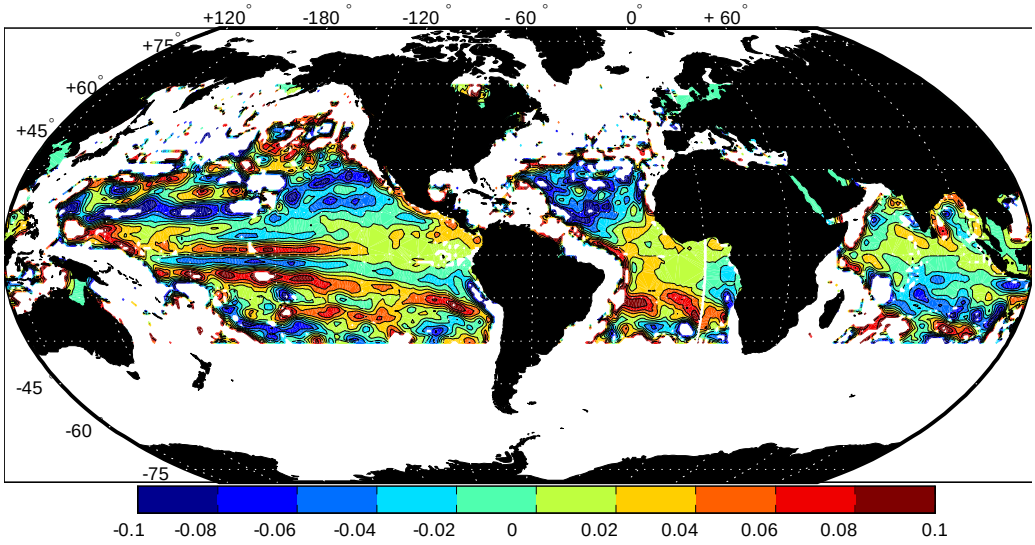

Figure 11: The difference $f/\beta w_E - V_g$ in Sverdrups per degree of zonal separation where the absolute value is less than 0.1Sv and $|w_{\min}| < 10^{-8}$m/s. (Same as Fig. 10 except that the difference is not normalized.)

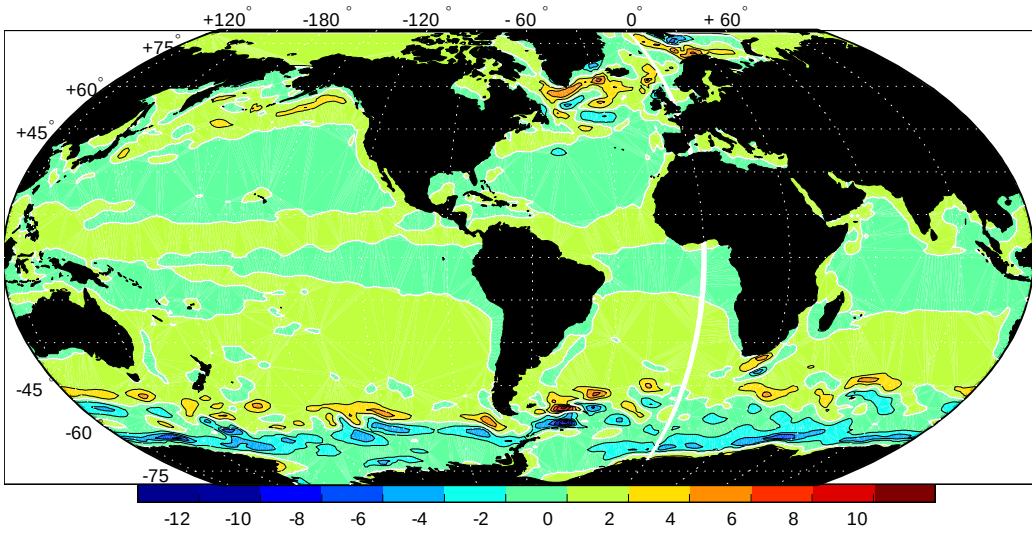

Figure 12: Mean wind stress curl, $(\Delta x/\beta)\,\nabla \times \boldsymbol{\tau}$, in Sverdrups, averaged over 5° of latitude and longitude.

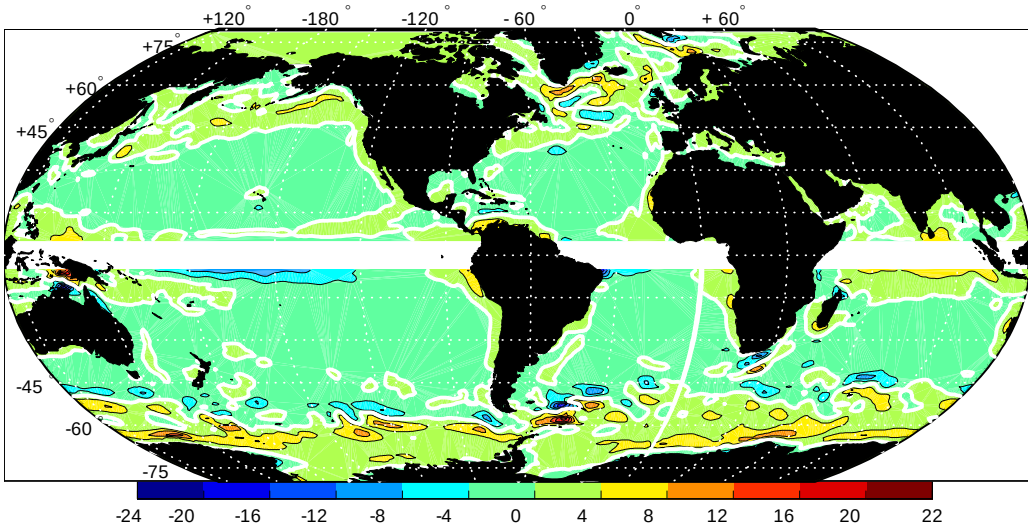

Figure 13: $10^6 \hat{\mathbf{k}} \cdot \nabla \times (\boldsymbol{\tau}/\rho_0 f)$ m/s, the Ekman pumping velocity as computed directly from the ECCO adjusted wind stress (m/s). Equatorial singularity has been suppressed. Compare to Fig. 4.